# Genomic characteristics, pathogenicity and viral shedding of a novel DVEV variant derived from goose

Zhanbao Guo,* Shuai Zhang,[†,‡,§] Yonglin Sun,[†,‡,§] Qiuyue Li,[†,‡,§] Yi Tang,[†,‡,§] Youxiang Diao,[†,‡,§] and Shuisheng Hou[*,1]

*Institute of Animal Sciences of Chinese Academy of Agricultural Sciences, Hai'dian, Beijing, 100097, China; [†]College of Animal Science and Technology, Shandong Agricultural University, Tai'an, Shandong Province, 271018, China; [‡]Shandong Provincial Key Laboratory of Animal Biotechnology and Disease Control and Prevention, Tai'an, Shandong, 271018, China; and [§]Shandong Provincial Engineering Technology Research Center of Animal Disease Control and Prevention, Tai'an, Shandong, 271018, China

**ABSTRACT** Duck virus enteritis (**DVE**), caused by the DVE virus (**DVEV**), is an acute, septicemic, and contagious disease affecting ducks of different breeds, ages, and sexes. In late spring and summer 2019, several outbreaks of DVE were reported in areas with large waterfowl industries in central and southern China. A goose farm located in Jining County, Shandong Province, was impacted by an acute DVE outbreak in July 2019. The causative DVEV field strain (Goose/DVEV/SDJN/China/2019) was subsequently isolated from the liver specimens collected from acute cases of dead geese, which showed severe hemorrhagic lesions on the esophageal mucosal membranes of specimens collected from all the postmortem cases. Comparison of the genome sequence of this newly isolated field strain (Goose/DVEV/SDJN/China/2019) with the common DVEV strains revealed insertions or mutations in the gB and gC genes, which possibly caused the observed high morbidity and mortality in this acute outbreak. We conducted a trial among geese to evaluate the pathogenicity of this strain. Healthy experimental goslings aged 15 d old were inoculated with $10^{-5.53}$ $ELD_{50}/0.2$ mL doses orally or through intramuscular injection. Clinical signs and esophageal erosion appeared in infected geese. Necropsy revealed hemorrhage and necrosis of the cloacal mucosa and liver. Detection of the virus using real-time PCR in the liver, brain, and spleen indicated that they were the hotspots of DVEV infections. One day after the DVEV infection, virus release and seroconvert were observed in infected geese. Thus, our studies demonstrate that DVEV is highly pathogenic and contagious in geese. To the best of our knowledge, this is the first study on the pathogenicity of mutant duck viral enteritis virus in goslings. This study serves as a foundation for further investigations into the pathophysiology of the recently identified variant DVEV strains.

Key words: duck virus enteritis, variant strain, goslings, pathogenicity analysis

## INTRODUCTION

Duck viral enteritis (**DVE**), also known as Duck plague (**DP**), is an acute and highly contagious disease in waterfowl. The characterized lesions of DVE include vascular damage, tissue hemorrhage, eruptions on the digestive mucosa, lesions in the lymphoid organs, and degenerative changes in parenchymatous organs (Shawky and Schat, 2002). Duck mortality usually begins 1 to 5 d after the onset of clinical signs and is more pronounced in breeding adult ducks (Dhama et al., 2017). Because of high mortality (80−100%), morbidity, and decreased egg production, this disease has caused severe economic losses in domestic waterfowl worldwide. The first case of DVE in domestic ducks was reported in the Netherlands in 1923 (Woźniakowski and Samorek-Salamonowicz, 2014). In China, the first DVE case was reported by Huang et al. in 1957 (Li et al., 2016), and subsequent DVE outbreaks were reported in recent years. Along with the rapid growth of the waterfowl industry, DVE outbreaks have been reported in several countries (Davison et al., 1993; Salguero et al., 2002), including North America (Leibovitz and Hwang, 1968), Canada, and France (Cai et al., 2010).

Duck viral enteritis virus (**DVEV**), the causative pathogen of DVE (Aravind et al., 2015), is an enveloped, double-stranded DNA virus belonging to the Anatid

herpesvirus 1 in the subfamily alphaherpesvirinae (Wu et al., 2012) according to the Eighth International Committee on the Taxonomy of Viruses (Fauquet and Fargette, 2005), although it has not been allocated to any genus. The G+C content of DVEV is 64.3%, which is higher than that of any other reported avian herpesvirus in the subfamily alpha herpesvirinae (Gardner et al., 1993). Because of the movement of migratory waterfowl across and between continents, the disease has been distributed globally (Dhama et al., 2017). According to reports, DVEV may spread horizontally between farmed and free-ranging birds (Woźniakowski and Samorek-Salamonowicz, 2014). As with many other herpesviruses, DVEV also has a latency state of latency. However, if DVEV is reactivated, an outbreak of the disease in susceptible duck farms may occur. The incubation period of DVEV is usually 3 to 7 d but can sometimes be as long as 14 d (Campagnolo et al., 2001). Thus, it is difficult to monitor and control the disease (Burgess et al., 1979). Although some vaccines have been developed, including naturally apathogenic or attenuated DVEV strains, the disease has not been controlled fully (Dhama et al., 2017). Currently, effective and reliable detection methods, such as viral isolation from chicken (**CEF**) or duck embryo fibroblasts (**DEF**), electron microscopy, and serological tests including enzyme-linked immunosorbent assay (**ELISA**), polymerase chain reaction (**PCR**), and loop-mediated isothermal amplification (**LAMP**) (Plummer et al., 1998; Hansen et al., 1999; Wu et al., 2011; Ferguson-Noel et al., 2012; Zhou et al., 2020) have been developed for the identification of the virus. Among these, the chicken and duck embryo cell cultures after infection with DVEV produce characteristic eosinophilic intranuclear inclusions (Plummer et al., 1998; Parida et al., 2004). All isolated DVEV strains currently belong to the same serotype (Dhama et al., 2017).

Multiple reports on DVE cases or outbreaks, as well as research articles on the molecular biology and pathogenicity of DVEV in ducklings, have been published (He et al., 2011; Li et al., 2011). However, the pathogenicity of DVEV in geese has not been extensively studied. Therefore, the present study aimed to investigate the pathogenicity of DVEV infection in the organs of geese. We isolated a DVEV strain (named Goose/DVEV/SDJN/China/2019) from a case of DVEV infection in a goose flock located in the Jining county of Shandong Province. In this article, we report our findings of the isolation and characterization of a novel DVEV field strain, as well as the clinical symptoms, pathological changes, and viral distribution in the organs of geese experimentally infected with this strain.

## MATERIALS AND METHODS

### Ethics Statement

All experiments with animals followed the applicable international, national, and institutional guidelines for the care and use of animals to minimize suffering. The Committee on the Animal Ethics of Shandong Agricultural University approved the study. The approved guidelines were respected to carry out the experiments.

### Sample Collection and Processing

The DVEV used in this study was isolated from a goose flock infected with DVEV in the Jining county of Shandong Province. The mortality rate of the flock was about 90%, with infected geese showing a severe hemorrhagic lesion on esophageal mucosal membranes in all postmortem cases. Twenty liver specimens from acute cases of dead geese were collected and homogenized in physiological saline and filtered through a 0.22 $\mu$m filter.

### Viral isolation and Titration of DVEV on Duck Embryos

Under aseptic conditions, the filtrate was inoculated on the chorioallantoic membrane of 9-day-old SPF duck embryos. At 96 h postinoculation, the chorioallantoic membrane was harvested under aseptic conditions, and the virus was passaged thrice (Wei et al., 2019; An et al., 2020; Jiang et al., 2021). The 50% egg lethal doses (ELD$_{50}$) of the isolated virus in duck embryos was calculated using the Reed and Muench method (Reed and Muench, 1938).

The DVEV-SDJN strain was cultivated in the chorioallantoic membranes of duck embryos, which were not infected with other common duck viral pathogens, including avian influenza A virus (**AIV**) (Starick et al., 2000), fowl adenovirus (**FAV**) (Sun et al., 2019), new goose parvovirus (**NGPV**) (Chen et al., 2016), duck viral hepatitis virus Ⅰ and Ⅲ (**DHAV-Ⅰ** and **DHAV-Ⅲ**) (Wang et al., 2019), tembusu virus (**TMUV**) (Sanisuriwong et al., 2020), duck reovirus (**DRV**) (Zhang et al., 2020), duck circovirus (**DuCV**) (Niu et al., 2018), newcastle disease virus (**NDV**) (Jang et al., 2011), and *Mycoplasma synoviae* (**MS**) (Ferguson-Noel et al., 2012).

### DNA Sequencing

Viral DNA was extracted from liver and spleen specimens using the TIANamp Genomic DNA Kit (TIANGEN biotech, Beijing, China). To confirm the presence of the virus, we used four pairs of specific primers (Table S1) to amplify the gB gene and the gC gene of DVEV. The primers specifically amplified a 3003-bp fragment of the gB gene and a 1296-bp fragment of the gC gene. PCR reactions were performed under the following conditions: initial denaturation at 94°C for 10 min, followed by 35 cycles of 94°C for 30 s, annealing at 60°C for 30 s, 72°C for 40 s, and a final elongation step at 72°C for 10 min. The PCR products were then analyzed using 1% agarose gel electrophoresis. Then, we cloned all PCR-positive products in the pMD18-T vector (TaKaRa,

Japan) and the recombinant plasmid was transformed into competent *DH5α E.coli* cells. The samples were then submitted to BGI (Company Ltd., Beijing, China) for sequencing using the Sanger dideoxy sequencing method. The SeqMan program of the DNAstar software package (version 7.1) (DNAstar, Madison, WI) was used to assemble the complete sequence of the gB and gC genes.

The complete sequences of the gB and gC genes were submitted to the GenBank database. The ClustalW method in the MegAlign program of the DNAstar software suite (version 8.13, DNAstar, Madison, WI) was used to align the complete sequence of the gB and gC genes with other available DVEV genome sequences to determine the nucleotide sequence homologies. We constructed a phylogenetic analysis of the nucleotide sequences based on the gB and gC genes using the MEGA6 software with the neighbor-joining method, in which, the bootstrap confidence values were 1,000 replicates (Tamura et al., 2013).

### Animal Experiments

Ninety healthy goslings aged 9 d old were obtained from a goose farm in Shandong Province, China. The goslings were kept in a cage until they were 15 d old. Before the start of the experiment, serum and cloacal swab samples from all geese were analyzed using ELISA and PCR, respectively, to confirm that they were free from DVEV infection.

The 90 healthy geese aged 15 d old were randomly divided into three groups, with 30 geese in each group. The study and control groups were housed in cages in separate rooms. For the preliminary experiment, geese in the 2 study groups were inoculated with 0.5 mL $10^{-5.53}$ $ELD_{50}/0.2$ mL of the challenge virus via oral and intramuscular routes, respectively. In the control groups, geese were inoculated with equal doses of phosphate-buffered saline (**PBS**) in the same manner. The feeding and management of these experimental geese were performed according to the established national procedures and biosecurity guidelines. Later, all geese were continuously observed daily for 21 d and clinical symptoms such as swollen head, photophobia, tearing, and mortality were recorded following infection.

Three geese in each group were euthanized by $CO_2$ on d 1, 3, 5, 7, 9, 14, and 21 following infection. Blood samples and cloaca samples were taken prior to euthanization. Various tissue specimens were collected from the liver, pancreas, esophagus, stomach, intestine, thymus, spleen, bursa, heart, lung, trachea, kidney, and brain. Tissue specimens from the control group were collected in the same manner. For pathological studies, each tissue specimen was split into two parts; one part was fixed in a 10% neutral formalin buffer, while the other was stored at −80°C for the viral load measurement test. At the end of the experiment, all remaining geese were euthanized for necropsy, and the gross lesions were recorded.

### Histopathology

After fixing tissues (liver, spleen, stomach, cloaca, heart, and pancreas) in a 10% neutral formalin buffer for 72 h after they were embedded in paraffin and then cut into 4 to 5-mm-thick sections. Subsequently, the sections were stained with hematoxylin and eosin for microscopic (Nikon, EclipseE100, Japan) to examination of histopathological changes.

### Detection of Viral Shedding and Viral Load by Real-Time Quantitative PCR

The viral DNA load in each tissue was determined using real-time quantitative PCR (**qPCR**). The primers and the TaqMan probe (Table S2) used to detect the viral load were designed based on the gB gene of the DVEV strain. The Applied Biosystems 7300 Fast Real-Time System (Applied Biosystems, Foster City, CA) was used to perform quantitative real-time PCR in a 96-well plate with the Premix Ex TaqTM kit (TaKaRa, Dalian, China). The 20 $\mu$L PCR mixture used for the real-time PCR analysis contained 10 $\mu$L of Premix Ex Taq (Probe qPCR) (2X), 0.4 $\mu$L of PCR forward primer, 0.4 $\mu$L of PCR reverse primer, 0.8 $\mu$L of the probe, 0.4 $\mu$L of ROX reference dye, 2 $\mu$L of DNA templates, and 6 $\mu$L of sterilized deionized water. The qPCR reactions were performed under the following conditions: initial denaturation at 95°C for 30 s, followed by 40 cycles of 95°C for 5 s and 60°C for 34 s. During the extension step, fluorescent signals were collected. All quantitative PCR reactions were analyzed in triplicate and repeated at least twice. The target fragment was cloned into the pMD18-T vector (TaKaRa, Beijing, China) to construct a standard recombinant plasmid. A standard curve was generated using a serial dilution of the standard plasmid ($1 \times 10^{-1}$ to $1 \times 10^{-7}$) copies per mL.

### Statistical Analysis

All data were presented as mean ±standard deviation (SD). Student's t-test was used to compare the mean body weights of different groups. One-way analysis of variance (ANOVA) with Tukey's post-test was used to compare the viral load in different organs and serum antibody titers. The statistical software GraphPad Prism (GraphPad Software Inc.) was used for statistical analysis. Statistical significance was set at $P < 0.05$ or $P < 0.01$.

## RESULTS

### Viral Identification and Sequence Analysis

Duck embryos inoculated with the DVEV field strain died within 5 dpi (days postinfection) (Table S3), showing symptoms of stunted growth and hemorrhagic lesions (Figure 3A, B). The allantois tested positive for DVEV by PCR, followed by sequence alignment and

phylogenetic analysis. The DVEV strain was named Goose/DVEV/SDJN/ China/2019. The propagated DVEV-SDJN strain used in this study was measured as $10^{-5.53}/0.2$ mL $ELD_{50}$.

The gB (GenBank accession number: ON996918) and gC (GenBank accession number: ON996919) genomes of the SDJN strain were compared with the reference Livestock and Gallid herpesvirus strains, respectively. Notably, the gB genome of the SDJN strain shared 99.6% to 100% sequence similarity with the UL27 (EF554401), FJ47 (MH778929), CHv (EF608147), and C-KCE (JN790941) strains, while the deduced amino acid sequences of the gB protein of the SDJN strain shared 99.7% to 100% identity (Table 1). The gC genome of the SDJN strain shared 99.6% to 99.8% sequence similarities with the C (EF607617), DEV (EF683582), CHv (JQ647509), CV (JQ673560), and CV C20E85 (KU216226) strains, while the nucleotide sequence homology was 99.4% to 99.8% (Table 2). The findings indicated that the gB and gC genes of the isolates could exhibit insertions or mutations. The gB gene had 4 distinct mutations (L238H, R378P, D465G, and M906V), while the gC gene had 2 specific alterations (Y102H and R368C) when compared to other strains. Surprisingly, 2 gene insertions were found in the gB genome, which may have caused the increased pathogenicity of this strain (Table 3). A phylogenetic tree was constructed based on the gB and gC gene sequence of the SDJN strain and the reference Livestock and Gallid herpesvirus strains. The results revealed that SDJN was clustered with Anatid herpesvirus 1 (Figure 1). Moreover, the phylogenetic tree also included Equid alphaherpesvirus 4, Gallid herpesvirus 1, Equid gammaherpesvirus 2, Gallid alphaherpesvirus 2, Equid gammaherpesvirus 5, Bovine alphaherpesvirus 1, and Suid alphaherpesvirus 1.

**Table 1.** Sequence distances of gB genome and proteins between Goose/DPV/SDJN/China/2022 and herpes virus species.

| Classification | gB genome | | | |
| | Virus strains | GeneBank No. | nt | aa |
| --- | --- | --- | --- | --- |
| Anatid alphaherpesvirus 1 | UL27 | EF554401 | 99.6 | 99.7 |
| | CHv | EF608147 | 99.9 | 99.9 |
| | FJ47 | MH778929 | 100 | 100 |
| | C-KCE | JN790941 | 100 | 100 |
| Gallid herpesvirus 1 | Jiangsu-2012-1 | KC248140 | 38.4 | 38.0 |
| | Tunisia/172/14 | KY131964 | 52.1 | 40.1 |
| Gallid alphaherpesvirus 2 | MD/HYD/18/007 | MK388080 | 28.7 | 9.2 |
| Equid herpesvirus 4 | L4-TR2011 | JN982955 | 56.9 | 58.2 |
| | VRLCU-412-2015 | KP699582 | 55.2 | 54.6 |
| | Fawzy | KX866264 | 55.2 | 55.4 |
| Equid gammaherpesvirus 2 | M14 | MK894598 | 41.9 | 32.1 |
| Equid gammaherpesvirus 5 | EGHV5.M4 | MK904568 | 28.7 | 10.0 |
| Bovine alphaherpesvirus 1 | XT-IBRV | MF287966 | 28.7 | 11.7 |
| | IBRV-4T3-1 | KY348790 | 30.2 | 47.8 |
| Suid alphaherpesvirus 1 | HLJ-D1 | MK248957 | 25.0 | 47.3 |

**Table 2.** Sequence distances of gC genome and proteins between Goose/DPV/SDJN/China/2022 and herpes virus species.

| Classification | gC genome | | | |
| | Virus strains | GeneBank No. | nt | aa |
| --- | --- | --- | --- | --- |
| Anatid alphaherpesvirus 1 | C | EF607617 | 99.6 | 99.4 |
| | DEV | EF683582 | 99.6 | 99.4 |
| | CV p80 | KJ549663 | 99.8 | 99.8 |
| | CV C20E85 | KU216226 | 99.8 | 99.8 |
| | CV | JQ673560 | 99.8 | 99.8 |
| | CHv | JQ647509 | 99.8 | 99.8 |
| Gallid herpesvirus 1 | 632 | U06635 | 27.5 | 12.8 |
| | K317 | JN969112 | 30.1 | 13.0 |
| Gallid alphaherpesvirus 2 | 05-X | AY129975 | 32.2 | 22.8 |
| | UVAS-IV | MN923520 | 36.5 | 23.2 |
| Equid herpesvirus 4 | CMVL 13539 | KY204084 | 42.9 | 13.7 |
| Bovine alphaherpesvirus 1 | TGM | KY748022 | 29.0 | 12.4 |
| | TR | MK659888 | 32.7 | 13.3 |
| Suid alphaherpesvirus 1 | AUJ | MN590223 | 26.0 | 8.4 |

## Clinical Symptoms and Gross Lesions of Experimental Geese

No clinical symptoms or gross lesions were observed in geese in the control group. Compared to the control group, DVEV-SDJN could significantly inhibit the weight gain of the infected ducklings following inoculation with the virus. The inhibitory effect was more pronounced in the injection group than that in the oral administration group (Figure 2A). After 21 d of infection, the weight of geese in the intramuscular injection group (691 g) was approximately half that of the control group (1208 g), while that in the oral administration group was 900 g. The morbidity of the infection group was 100%, while the mortality rate of the goslings was higher, at 40% in the orally administered group and 46.7% in the injection group (Figure 2B). The clinical signs of the intramuscular injection group and the orally administered group were similar after inoculation. Geese from the infected groups exhibited typical symptoms of DVEV at 3 days post-inoculation (dpi), including apathy, retracted neck, appetite loss, increased thirst, feather loss, and matte, drooping wing, movement disorder, swelling of the head and neck, swollen eyelids, tears, and corneal opacification, as well as greenish diarrhea (Figure 3C−F). Moreover, severely infected ducks also showed dyspnea, ataxia, paralysis, and a green foul-smelling liquid discharge from the mouth and nose (Figure 3G).

After observation, the pathological changes of the orally administered group and the injection group were the same, and the symptoms in the experimental geese were consistent with those of the naturally infected group. The examined liver exhibited necrosis and bleeding in the virus-infected geese (Figure 3H). In addition, the significant histopathological changes observed in the buccal and esophageal mucosa of SDJN-inoculated birds were diffuse hemorrhages (Figure 3I). In the meantime, we observed a prominent bleeding band at the junction of the hypertrophied esophagus and glandular stomach (Figure 3M). Moreover, the examined monogastric corpuscles obtained from geese inoculated with SDJN

**Table 3.** Amino acid alterations of the DPV SDJN isolates contribute to enhanced replication, pathogenicity, and transmissibility in waterfowls.

| Virus strains | gB | | | | | | Virus strains | gC | |
|---|---|---|---|---|---|---|---|---|---|
| | 238 | 378 | 397-402 | 465 | 708-713 | 906 | | 102 | 368 |
| SDJN | L | R | LEAPEF | D | LERPEF | M | SDJN | Y | R |
| FJ47 | L | R | - | D | - | M | C | H | C |
| UL27 | H | P | - | G | - | M | DEV | H | C |
| C-KCE | L | R | - | D | - | M | CHv | Y | C |
| CHv | L | R | - | D | - | V | CV | Y | C |

revealed hemorrhagic spots and necrotic foci (Figure 3N). Severe pathological damage was observed in the intestines of geese inoculated with SDJN and the examination showed hemorrhage and congestion of the intestinal mucosa with grayish-yellow pseudomembranous necrotic foci (Figure 3K and L). Examination of the cloacal cavity of infected geese revealed necrosis and bleeding (Figure 3J). A yellowish transparent liquid was observed in the subcutaneous tissue of the swollen head and neck (Figure 3O). Other symptoms in geese inoculated with SDJN included severe lesions characterized by hyperemia and congestion in the lungs (Figure 3Q), hemorrhage of the endocardium and epicardium (Figure 3S), splenomegaly (Figure 3P), and hemorrhage in the bursa of Fabricius (Figure 3R).

## Histopathology

Pathological changes were detected in various tissues in the infected geese. The liver cells displayed diffuse fatty degeneration and focal necrosis of hepatocytes (Figure 4A). Hemorrhage was observed in the liver with massive inflammatory cell infiltration (Figure 4B). Bleeding was observed in the spleen (Figure 4C). There were necrotic lesions of different sizes and inflammatory cell infiltration (Figure 4D). Severe alterations were observed in the digestive tract of geese inoculated with SDJN. These alterations summarized as myogastric, showed horny membrane damage and sub-keratinous hemorrhage (Figure 4E).

Myogastric mucosal bleeding, necrosis, and exfoliation of epithelial cells were observed. Inflammatory cells and necrosis were observed on the surface of the mucous membrane. Hyperemia and inflammatory cell infiltration in lamina propria (Figure 4F) were evident. Bleeding and inflammatory cell infiltration were recorded at the junction of the adenogastric and myogastric junctions (Figure 4G). The glandular stomach showed tissue necrosis and destruction of the structure as well as interstitial hyperemia with inflammatory cell infiltration (Figure 4H) was observed. The chorionic membrane showed rupture and necrosis (Figure 4I). The outer cloaca was filled with several red blood cells and inflammatory cell infiltration (Figure 4J). The outer mucosa of the cloaca was destroyed and showed necrosis (Figure 4K). Furthermore, the heart was full of red blood cells and showed inflammatory cell infiltration (Figure 4L). Rupture of the myocardial fibers, increased gap, and inflammatory cell infiltration (Figure 4M, N) were observed. The pancreas was filled with red blood cells and showed necrosis and inflammatory cell infiltration (Figure 4O).

## Detection of Viral Load in Tissues

qPCR was used to assess the levels of viral DNA in different tissues (Table S4). All samples in the infection group tested positive for the virus at 1 dpi in the evaluated organs, whereas no viral RNA was found in the control group (Figure 5). The viral load in the liver, spleen,
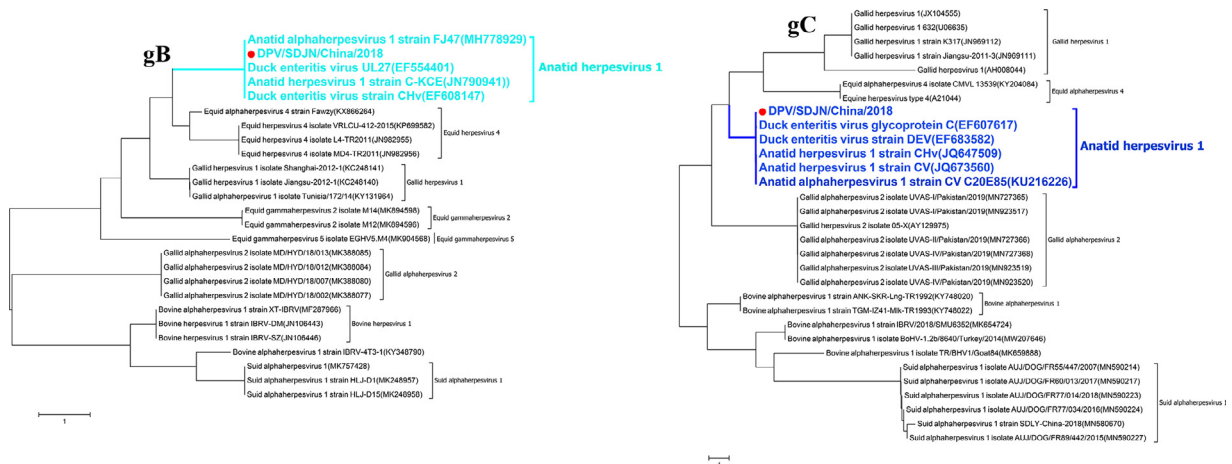


**Figure 1.** Phylogenetic studies based on the gB and gC amino acid sequences of DVEV-SDJN strains and other DVEVs. The trees were created using the Neighbor-joining method with 1000 bootstrap replicates and MEGA 7.0 software. A red dot designates the DVEV-SDJN isolate identified in this study.
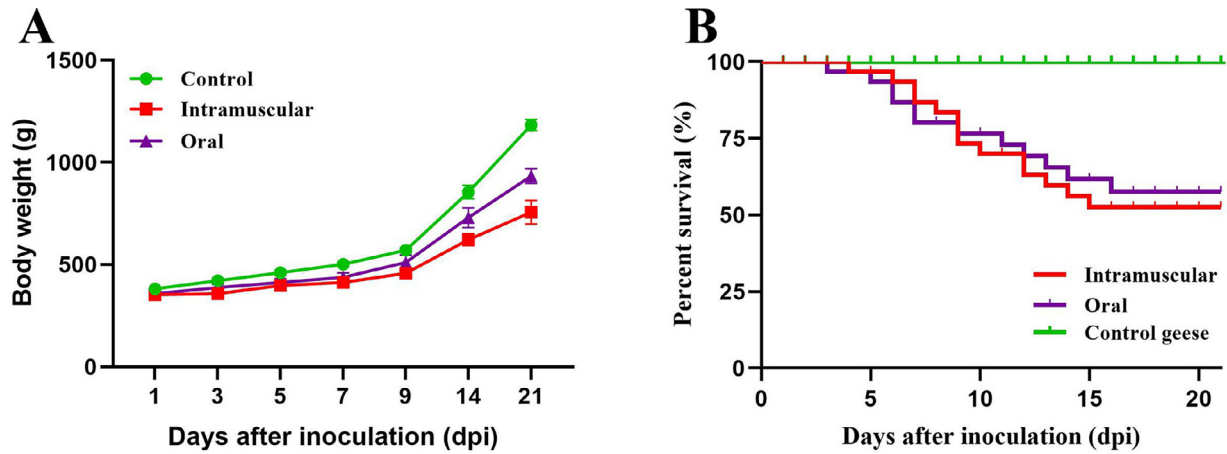
**Figure 2.** Body weight gain and survival curves after DVEV-SDJN infection. (A) Weight gain of goslings infected with DVEV-SDJN. (B) Survival curves of goslings after infection with DVEV-SDJN.

brain, and esophagus (Up to 10.75, 12.13, 10.07, and 10.09 copies (log10)/$\mu$gDNA, respectively) was significantly higher than that in other organs during the trial. Notably, DVEV multiplies quickly and abundantly in the brain, indicating that it can cross the blood-brain barrier (Figure 5G, H). Three days after inoculation, the amount of viral DNA in the digestive system increased rapidly (Up to 9 copies (log10)/$\mu$gDNA or more) and remained at a high level 21 d later (Figure 5C, D), which was consistent with the presence of severe digestive tract lesions following DVEV infection. Different tissues showed elevated DVEV loads at 3 dpi, which all tissues showed considerably higher loads at 5 dpi. Moreover, when these two infection groups were compared, more viral copies were observed in the tested tissues of the injection than those in the oral administration group. Our findings collectively indicate that DVEV could easily invade and replicate in various tissues, including the

digestive tract. We also observed the shedding of virus from the cloaca and viral blood transformation in the infected goslings at 1 dpi by identifying the viral DNA in the blood and cloaca at 1, 3, 5, 7, 9, 14, and 21 dpi, whereas the control group goslings consistently tested negative for DVEV (Figure 5I, J).

## DISCUSSION

DVE is one of the most severe and deadly illnesses affecting waterfowl (Anseriformes), including geese, ducks, and swans(Kaleta, 1990). The causative agent, DVEV, also known as anatid herpesvirus 1, is a member of the genus Mardivirus and the family Herpesviridae (Lefkowitz et al., 2018). The viral genome consists of about 160 kb of double-stranded linear DNA and is organized into three distinct regions: a unique long (**UL**), a unique short (**US**), and a unique short internal repeat
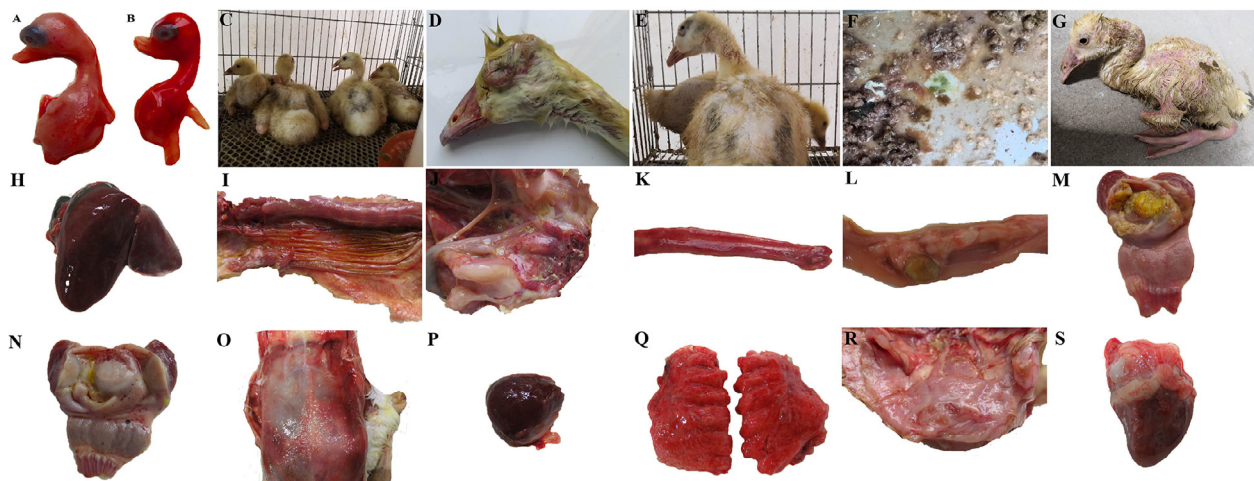


**Figure 3.** Duck embryos and goslings with DVEV-SDJN infection displaying clinical symptoms and pathological changes. (A) Uninfected duck embryos. (B) Stunting and embryo bleeding were in the duck embryos used to isolate the DVEV virus. (C) Infected geese exhibit depressive symptoms, neck tightness, dyskinesia, respiratory difficulty, and green, foul-smelling fluid coming from their mouths and noses. (D) Infected geese have a swollen head, enlarged eyelids, and lacrimation. (E) Infected geese have clouded corneas, lost their shine, and lost their feathers. (F) Green feces are excreted by sick geese. (G) Infected geese exhibit ataxia, paralysis, and green, rancid fluid coming from their mouths and noses. (H) Bleeding and necrosis in the liver. (I) Widespread esophageal bleeding. (J) Myogastric hemorrhage and necrosis. (K-L) The intestinal mucosa is hemorrhagic and engorged, together with grayish-yellow foci of pseudomembranous necrosis. (M) Bleeding at the esophageal-gastrointestinal junction. (N) Cloacal necrosis and bleeding. (O) Skin tissue containing a light yellow translucent fluid. (P) Bleeding from the spleen. (Q) Bleeding and congestion in the lungs. (R) Bursal hemorrhage. (S) Epicardial hemorrhage.
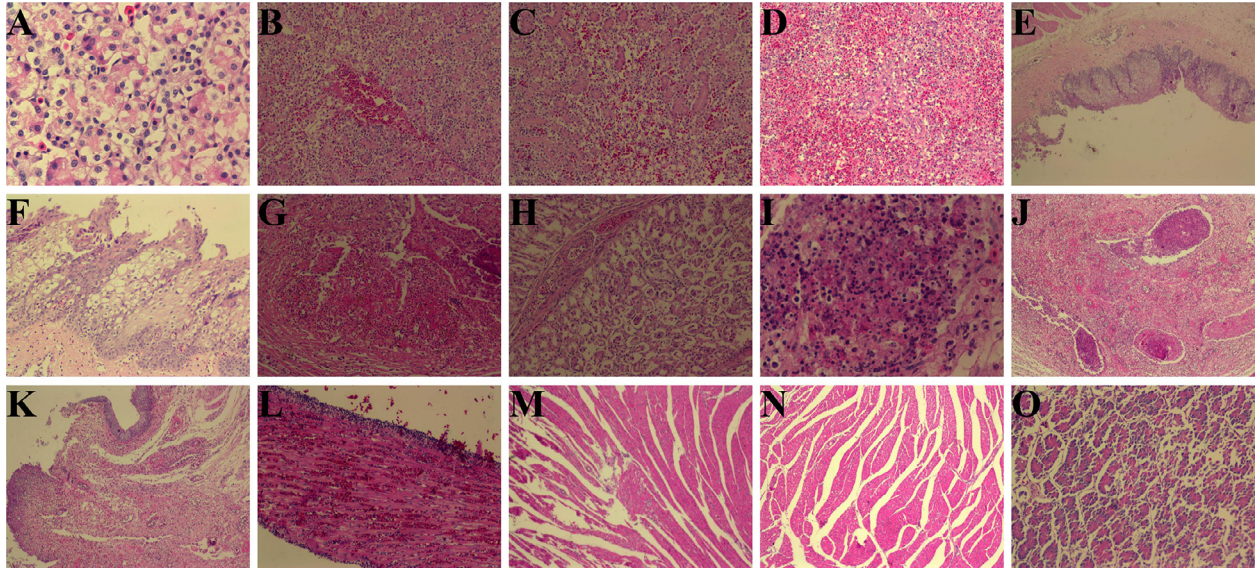
**Figure 4.** Photomicrographs of histological H&E-stained of goslings. (A) Hepatocellular steatosis and focal necrosis (HE × 400). (B) Hemorrhage in the liver with massive inflammatory cell infiltration (HE × 100). (C) Bleeding in the spleen (HE × 100). (D) Parenchymal presence of necrotic lesions and inflammatory cell infiltration in the spleen (HE × 100). (E) Myogastric corneal injury and subkeratinous hemorrhage (HE × 40). (F) Myogastric mucosa was hemorrhagic, epithelial cells were necrotic and detached, there were a lot of inflammatory cells and necrotic material in the superficial layer of mucosa, and the lamina propria was congested and inflammatory cells infiltrated (HE × 100). (G) Hemorrhage at the junction of the glandular and muscular stomach with inflammatory cell infiltration (HE × 100). (H) Glandular stomach tissue necrosis, structural destruction, interstitial congestion, inflammatory cell infiltration (HE × 100). (I) The cloaca was filled with a large number of erythrocytes, infiltrated by inflammatory cells, and the chorionic villus was broken and necrotic (HE × 400). (J) The cloaca was filled with a large number of erythrocytes, infiltrated by inflammatory cells, and the chorionic villus was broken and necrotic (HE × 100). (K) The extra-cloacal intestinal mucosa was disrupted, necrotic, and filled with a large number of red blood cells (HE × 40). (L) Heart filled with numerous erythrocytes and infiltrated with inflammatory cells (HE x 100). (M) Myocardial fiber disruption, and inflammatory cell infiltration (HE × 40). (N) Increased myocardial fiber gap (HE × 400). O. Pancreas filled with a large number of erythrocytes, necrosis, and inflammatory cell infiltration (HE × 100).

(**IRS**) and short terminal repeat (**TRS**) region. At least 67 genes in the DVEV genome are homologous to those in other members of the subfamily Alphaherpesvirinae. Over 48 bird species are possibly vulnerable to DVEV infection (Leibovitz, 1968; Brand and Docherty, 1984; Kaleta, 1990). The Netherlands reported the first DVEV infection among domestic ducks in 1923 (Cheng et al., 2002). China has had several outbreaks of DVEV-caused illness in waterfowl species. The prevalence of asymptomatic carriers of this virus makes it possible to miss the clinical manifestations of the disease (Wobeser, 1987; Gough and Alexander, 1990). Given that mortality rates, particularly for young birds, can reach 100%, DVE has a significantly negative economic impact on the care of waterfowl.

A viral illness that seriously harms to the digestive tract has been spreading across waterfowl farms in several eastern provinces of China since May 2019. Compared to the traditional DVE, this new infectious illness has more significant rates of morbidity and mortality, with an expanding epidemic range. In the current work, DVEV and many other waterfowl viruses were isolated and propagated using SPF duck embryos (Johnson and Heneine, 2001; Worku et al., 2022). Clinical samples collected from this epidemic DVEV outbreak at a goose farm in Shandong province were used to successfully isolate the virus. Through three serial duck embryo passages, the recovered DVEV isolates yielded a titer of $10^{-5.53}$ TCID$_{50}$/mL, which produced the characteristic

cytopathic effects (**CPE**) of clumping and fused cells in duck embryo fibroblast cell cultures. The entry of alpha herpes viruses entrance into receptive cells appears to be a complex process involving several types of interactions with the cell surface and at least four viral glycoproteins (Spear et al., 2000). The virus binds to heparan sulfate on the cell surface by the action of glycoproteins gB and/or gC. The molecular technique of PCR is a quick and accurate test to identify disease-carrying humans, as well as infections among various animals, including birds (Pritchard et al., 1999; Chen et al., 2013). PCR-based identification of two DVEV genes presented more evidence of the presence of viral DNA in the infected SPF duck eggs (gB and gC). Sequence similarity and phylogenetic analyses revealed that DPV-SDJN differed from one another in various ways. Insertions or mutations in the gB and gC genes of the DVEV-SDJN isolate may be responsible for the increased pathogenicity of this strain. However, there is a lack of systematic reports on the pathogenicity of the DVEV-SDJN strain in waterfowl. Therefore, a study on the pathogenicity of DVEV-SDJN is useful to further investigate the pathogenicity of DVEV, which is crucial for the proper management of the occurrence and spread of this virus.

In this study, we used healthy goslings to successfully establish an experimental model for DVEV infection to investigate the pathogenicity of DVEV in geese. The goslings in both the intramuscular injection and oral administration groups displayed similar clinical signs as
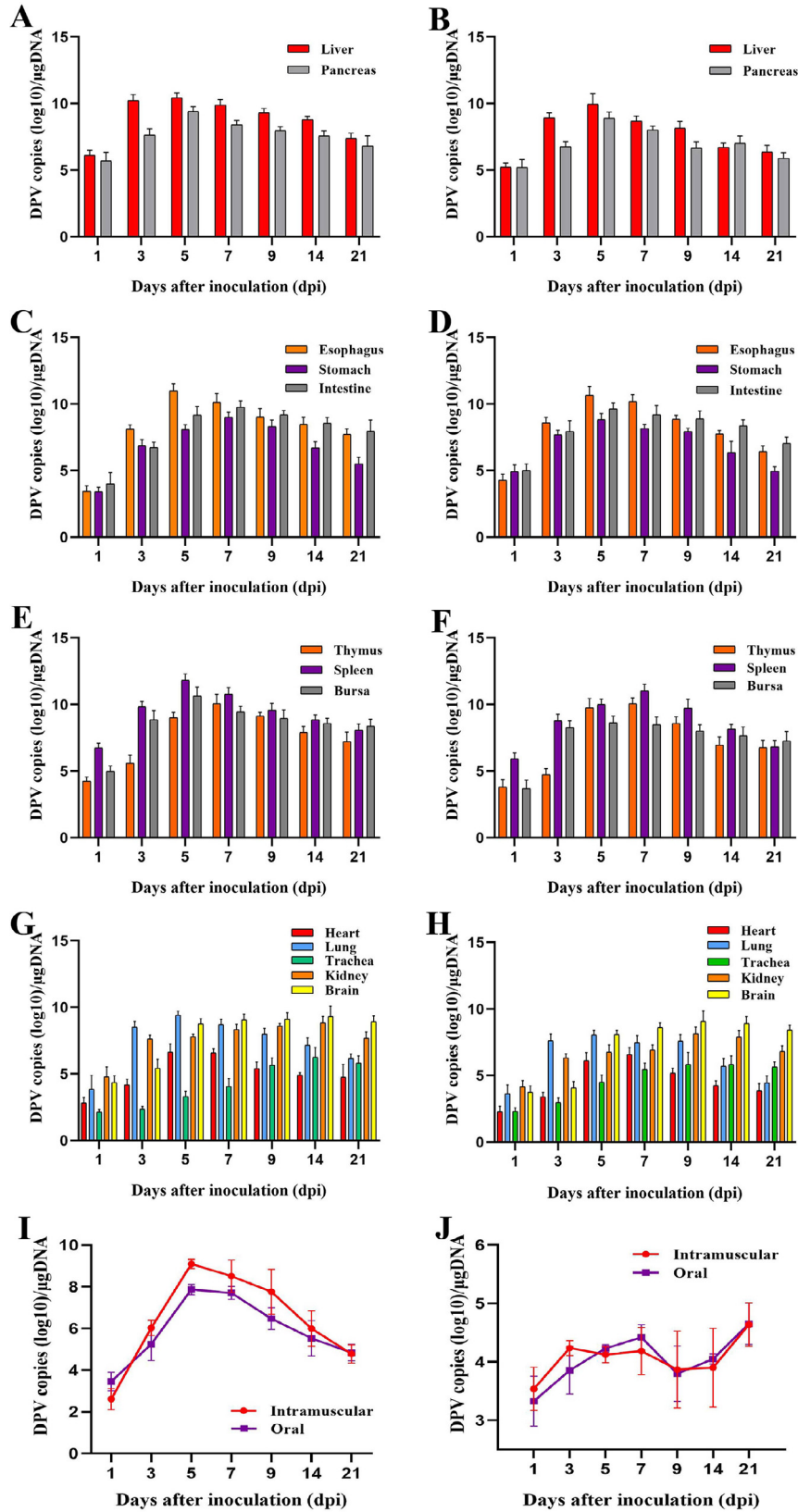
**Figure 5.** Detection of viral DNA content in organs. Intramuscular injection group (A) and oral group (B) of viral DNA detection in the digestive organs. Digestive tract viral DNA testing in the intramuscular group (C) and oral group (D). Intramuscular injection group (E) and oral group (F) of viral DNA detection in the Immune organ. Intramuscular injection group (G) and oral group (H) of viral DNA detection in the other organ. The rule for viral shedding in the cloaca (I) and blood (J).

those observed in outbreaks in wild birds. The mortality rate of goslings was higher, being 40% in the group that receiving the DVEV-SDJN orally and 46.7% in the group that receiving the injection, with 100% morbidity in the infection group. DVEV had broad tissue tropism in the infected geese and replicated rapidly in several tissues, especially the spleen, liver, brain, and digestive tract, causing serious pathological lesions. Another report demonstrated that the levels of DVEV in systemic organs had a close relationship with the progression of the disease (Xuefeng et al., 2008). In this study, different organs of the infected goose exhibited pathological alterations including edema, bleeding, necrosis, and tissue necrosis. The immune organs also underwent severe lymphocyte depletion and tissue necrosis. The main cause of the immune system's decline in waterfowl may be the nvasion of the virus in immunological organs, which makes them more susceptible to infection by other pathogens, eventually causing death (Ayalew et al., 2017). The pathogenic effects in the intramuscular injection and oral administration groups were essentially the same. Due to the action of several digestive enzymes in the digestive tract, oral inoculation can severely harm to the virus. Further research is required to determine the mechanism underlying the higher pathogenic effect of oral infection observed in this study. Following infection, DVEV DNA can be consistently found in the cloacal swabs and blood of the injection and oral administration groups. More extensive infection is caused by viral nucleic acids secreted from the cloaca, which contaminate food and water. DVEV can be transmitted vertically through blood. Widespread DVEV infection is directly associated with the shedding of the virus through the cloaca and blood, which also increases the possibility of practical methods to stop the spread of the illness. The spleen is the ideal organ to check for DVEV infection, along with a few other organs with significant viral loads, such as the liver and brain. The findings also demonstrated that the DVEV had a potent erosive effect on the spleen, thymus, bursa, and other immune organs, leading to immune organ malfunction, which may be the main cause of the secondary infection among ducks following DVEV infection. Although the detection of viral DNA in the brains demonstrates the ability of DVEV to easily cross the blood-brain barrier and produce depression in infected ducks, additional studies are needed to understand this process.

To the best of our knowledge, this is the first study on the pathogenicity of the mutant DVEV in goslings. This work serves as a foundation for further investigation into the pathophysiology of the recently identified mutant DVEV strain. The discrepancies between the reported strains and the DVEV-SDJN genome were also discussed in detail in our work. An efficient vaccination strategy is urgently needed for the prevention and control of the illness to counteract its persistence and prevalence. Further research is also necessary to understand the mechanism involved in the genetic changes and virulence of this virus.

## DISCLOSURES

The authors declare no conflict of interest.

## SUPPLEMENTARY MATERIALS

Supplementary material associated with this article can be found in the online version at doi:10.1016/j.psj.2022.102392.

## REFERENCES

An, D., J. Zhang, J. Yang, Y. Tang, and Y. Diao. 2020. Novel goose-origin astrovirus infection in geese: the effect of age at infection. Poultry Sci. 99:4323–4333.

Aravind, S., N. M. Kamble, S. S. Gaikwad, S. K. Shukla, S. Dey, and C. M. Mohan. 2015. Adaptation and growth kinetics study of an Indian isolate of virulent duck enteritis virus in Vero cells. Microb. Pathog. 78:14–19.

Ayalew, L. E., A. Gupta, J. Fricke, K. A. Ahmed, S. Popowich, B. Lockerbie, S. K. Tikoo, D. Ojkic, and S. Gomis. 2017. Phenotypic, genotypic and antigenic characterization of emerging avian reoviruses isolated from clinical cases of arthritis in broilers in Saskatchewan. Canada. Sci. Rep. 7:3565.

Brand, C. J., and D. E. Docherty. 1984. A survey of North American migratory waterfowl for duck plague (duck virus enteritis) virus. J. Wildl. Dis. 20:261–266.

Burgess, E. C., J. Ossa, and T. M. Yuill. 1979. Duck plague: a carrier state in waterfowl. Avian Dis. 23:940–949.

Cai, M., A. Cheng, M. Wang, W. Chen, X. Zhang, S. Zheng, Y. Pu, K. Lou, Y. Zhang, L. Sun, L. Wang, D. Zhu, Q. Luo, and X. Chen. 2010. Characterization of the Duck Plague virus UL35 gene. Intervirology 53:408–416.

Campagnolo, E. R., M. Banerjee, B. Panigrahy, and R. L. Jones. 2001. An outbreak of duck viral enteritis (duck plague) in domestic Muscovy ducks (Cairina moschata domesticus) in Illinois. Avian Dis. 45:522–528.

Chen, L. L., Q. Xu, R. H. Zhang, L. Yang, J. X. Li, Z. J. Xie, Y. L. Zhu, S. J. Jiang, and X. K. Si. 2013. Improved duplex RT-PCR assay for differential diagnosis of mixed infection of duck hepatitis A virus type 1 and type 3 in ducklings. J. Virol. Methods 192:12–17.

Chen, S., S. Wang, X. Cheng, S. Xiao, X. Zhu, F. Lin, N. Wu, J. Wang, M. Huang, M. Zheng, S. Chen, and F. Yu. 2016. Isolation and characterization of a distinct duck-origin goose parvovirus causing an outbreak of duckling short beak and dwarfism syndrome in China. Arch. Virol. 161:2407–2416.

Cheng, J. L., M. J. Bruno, J. J. Bergman, E. A. Rauws, G. N. Tytgat, and K. Huibregtse. 2002. Endoscopic palliation of patients with biliary obstruction caused by nonresectable hilar cholangiocarcinoma: efficacy of self-expandable metallic Wallstents. Gastrointest. Endosc. 56:33–39.

Davison, S., K. A. Converse, A. N. Hamir, and R. J. Eckroade. 1993. Duck viral enteritis in domestic muscovy ducks in Pennsylvania. Avian Dis. 37:1142–1146.

Dhama, K., N. Kumar, M. Saminathan, R. Tiwari, K. Karthik, M. A. Kumar, M. Palanivelu, M. Z. Shabbir, Y. S. Malik, and

R. K. Singh. 2017. Duck virus enteritis (duck plague) - a comprehensive update. Vet. Q. 37:57–80.

Fauquet, C. M., and D. Fargette. 2005. International Committee on Taxonomy of Viruses and the 3,142 unassigned species. Virol. J. 2:64.

Ferguson-Noel, N., V. A. Laibinis, and M. Farrar. 2012. Influence of swab material on the detection of Mycoplasma gallisepticum and Mycoplasma synoviae by real-time PCR. Avian Dis. 56:310–314.

Gardner, R., J. Wilkerson, and J. C. Johnson. 1993. Molecular characterization of the DNA of Anatid herpesvirus 1. Intervirology 36:99–112.

Gough, R. E., and D. J. Alexander. 1990. Duck virus enteritis in Great Britain, 1980 to 1989. Vet. Rec. 126:595–597.

Hansen, W. R., S. E. Brown, S. W. Nashold, and D. L. Knudson. 1999. Identification of duck plague virus by polymerase chain reaction. Avian Dis. 43:106–115.

He, Q., Q. Yang, A. Cheng, M. Wang, J. Xiang, D. Zhu, R. Jia, Q. Luo, Z. Chen, Y. Zhou, and X. Chen. 2011. Expression and characterization of UL16 gene from duck enteritis virus. Virol. J. 8:413.

Jang, J., S. H. Hong, and I. H. Kim. 2011. Validation of a real-time RT-PCR method to quantify Newcastle Disease Virus (NDV) titer and comparison with other quantifiable methods. J. Microbiol. Biotechnol. 21:100–108.

Jiang, X., Y. Lin, J. Yang, H. Wang, C. Li, X. Teng, Y. Tang, and Y. Diao. 2021. Genetic characterization and pathogenicity of a divergent broiler-origin orthoreovirus causing arthritis in China. Transbound. Emerg. Dis. 68:3552–3562.

Johnson, J. A., and W. Heneine. 2001. Characterization of endogenous avian leukosis viruses in chicken embryonic fibroblast substrates used in production of measles and mumps vaccines. J. Virol. 75:3605–3612.

Kaleta, E. F. 1990. Herpesviruses of birds—a review. Avian Pathol. 19:193–211.

Lefkowitz, E. J., D. M. Dempsey, R. C. Hendrickson, R. J. Orton, S. G. Siddell, and D. B. Smith. 2018. Virus taxonomy: the database of the International Committee on Taxonomy of Viruses (ICTV). Nucleic. Acids. Res. 46(D1):D708–D717.

Leibovitz, L. 1968. Progress report: duck plague surveillance of American Anseriformes. Wildl. Dis. 4:87–91.

Leibovitz, L., and J. Hwang. 1968. Duck plague on the American continent. Avian Dis. 12:361–378.

Li, L., A. Cheng, M. Wang, J. Xiang, X. Yang, S. Zhang, D. Zhu, R. Jia, Q. Luo, Y. Zhou, Z. Chen, and X. Chen. 2011. Expression and characterization of duck enteritis virus gI gene. Virol. J. 8:241.

Li, N., T. Hong, R. Li, M. Guo, Y. Wang, J. Zhang, J. Liu, Y. Cai, S. Liu, T. Chai, and L. Wei. 2016, 1-8. Pathogenicity of duck plague and innate immune responses of the Cherry Valley ducks to duck plague virus. Sci. Rep. 6.

Niu, X., L. Liu, C. Han, J. Li, and X. Zeng. 2018. First findings of duck circovirus in migrating wild ducks in China. Vet. Microbiol. 216:67–71.

Parida, M., G. Posadas, S. Inoue, F. Hasebe, and K. Morita. 2004. Real-time reverse transcription loop-mediated isothermal amplification for rapid detection of West Nile virus. J. Clin. Microbiol. 42:257–263.

Plummer, P. J., T. Alefantis, S. Kaplan, P. O'Connell, S. Shawky, and K. A. Schat. 1998. Detection of duck enteritis virus by polymerase chain reaction. Avian Dis. 42:554–564.

Pritchard, L. I., C. Morrissy, K. Van Phuc, P. W. Daniels, and H. A. Westbury. 1999. Development of a polymerase chain reaction to detect Vietnamese isolates of duck virus enteritis. Vet. Microbiol. 68:149–156.

Reed, L. J., and H. Muench. 1938. A simple method of estimating fifty per cent endpoints. Am. J. Epidemiol. 3:493–497.

Salguero, F. J., P. J. Sanchez-Cordon, A. Nunez, and J. C. Gomez-Villamandos. 2002. Histopathological and ultrastructural changes associated with herpesvirus infection in waterfowl. Avian Pathol. 31:133–140.

Sanisuriwong, J., N. Yurayart, A. Thontiravong, and S. Tiawsirisup. 2020. Duck Tembusu virus detection and characterization from mosquitoes in duck farms, Thailand. Transbound. Emerg. Dis. 67:1082–1088.

Shawky, S., and K. A. Schat. 2002. Latency sites and reactivation of duck enteritis virus. Avian Dis. 46:308–313.

Spear, P. G., R. J. Eisenberg, and G. H. Cohen. 2000. Three classes of cell surface receptors for alphaherpesvirus entry. Virology 275:1–8.

Starick, E., A. Romer-Oberdorfer, and O. Werner. 2000. Type- and subtype-specific RT-PCR assays for avian influenza A viruses (AIV). J. Vet. Med. B Infect. Dis. Vet. Public Health 47:295–301.

Sun, J., Y. Zhang, S. Gao, J. Yang, Y. Tang, and Y. Diao. 2019. Pathogenicity of fowl adenovirus serotype 4 (FAdV-4) in chickens. Infect. Genet. Evol. 75:104017.

Tamura, K., G. Stecher, D. Peterson, A. Filipski, and S. Kumar. 2013. MEGA6: Molecular Evolutionary Genetics Analysis version 6.0. Mol. Biol. Evol. 30:2725–2729.

Wang, A. P., L. Liu, L. L. Gu, S. Wu, C. M. Guo, Q. Feng, W. L. Xia, C. Yuan, and S. Y. Zhu. 2019. Expression of duck hepatitis A virus type 1 VP3 protein mediated by avian adeno-associated virus and its immunogenicity in ducklings. Acta Virol. 63:53–59.

Wei, Z., H. Liu, Y. Diao, X. Li, S. Zhang, B. Gao, Y. Tang, J. Hu, and Y. Diao. 2019. Pathogenicity of fowl adenovirus (FAdV) serotype 4 strain SDJN in Taizhou geese. Avian Pathol. 48:477–485.

Wobeser, G. 1987. Experimental duck plague in blue-winged teal and Canada geese. J. Wildl. Dis. 23:368–375.

Worku, T., M. Dandecha, D. Shegu, A. Aliy, and D. Negessu. 2022. Isolation and molecular detection of Newcastle disease virus from field outbreaks in chickens in Central Ethiopia. Vet. Med. (Auckl) 13:65–73.

Woźniakowski, G., and E. Samorek-Salamonowicz. 2014. First survey of the occurrence of duck enteritis virus (DEV) in free-ranging Polish water birds. Arch. Virol. 159:1439–1444.

Wu, Y., A. Cheng, M. Wang, Q. Yang, D. Zhu, R. Jia, S. Chen, Y. Zhou, X. Wang, and X. Chen. 2012. Complete genomic sequence of Chinese virulent duck enteritis virus. J. Virol. 86:5965.

Wu, Y., A. Cheng, M. Wang, S. Zhang, D. Zhu, A. B. Jia, B. Q. Luo, Z. Chen, and X. Chen. 2011. Serologic detection of duck enteritis virus using an indirect ELISA based on recombinant UL55 protein. Avian Dis. 55:626–632.

Xuefeng, Q., Y. Xiaoyan, C. Anchun, W. Mingshu, Z. Dekang, and J. Renyong. 2008. The pathogenesis of duck virus enteritis in experimentally infected ducks: a quantitative time-course study using TaqMan polymerase chain reaction. Avian Pathol. 37:307–310.

Zhang, S., W. Li, X. Liu, X. Li, B. Gao, Y. Diao, and Y. Tang. 2020. A TaqMan-based real-time PCR assay for specific detection of novel duck reovirus in China. BMC Vet. Res. 16.

Zhou, X., M. Wang, A. Cheng, Q. Yang, Y. Wu, R. Jia, M. Liu, D. Zhu, S. Chen, S. Zhang, X. X. Zhao, J. Huang, S. Mao, X. Ou, Q. Gao, Y. Liu, Y. Yu, L. Zhang, B. Tian, L. Pan, M. U. Rehman, and X. Chen. 2020. Development of a simple and rapid immunochromatographic strip test for detecting duck plague virus antibodies based on gI protein. J. Virol. Methods 277:113803.